



Published in final edited form as:

*Mol Cell*. 2010 December 10; 40(5): 787–797. doi:10.1016/j.molcel.2010.11.010.

## Oxidative protein folding by an endoplasmic reticulum localized peroxiredoxin

Ester Zito<sup>1</sup>, Eduardo Pinho Melo<sup>1,5</sup>, Yun Yang<sup>1</sup>, Åsa Wahlander<sup>1</sup>, Thomas A. Neubert<sup>1,4</sup>, and David Ron<sup>1,2,3,6,7</sup>

<sup>1</sup> Kimmel Center for Biology and Medicine of the Skirball Institute, New York University School of Medicine, New York, New York 10016 USA

<sup>2</sup> Department of Cell Biology, New York University School of Medicine, New York, New York 10016 USA

<sup>3</sup> Department of Medicine, New York University School of Medicine, New York, New York 10016 USA

<sup>4</sup> Department of Pharmacology, New York University School of Medicine, New York, New York 10016 USA

<sup>5</sup> Institute for Biotechnology and Bioengineering, Centre for Molecular and Structural Biomedicine, Universidade do Algarve, Portugal

<sup>6</sup> Institute of Metabolic Sciences, University of Cambridge, Cambridge CB2 0QQ, UK

### Abstract

Endoplasmic reticulum (ER) oxidation 1 (*ERO1*) transfers disulfides to protein disulfide isomerase (PDI) and is essential for oxidative protein folding in simple eukaryotes such as yeast and worms. Surprisingly, *ERO1*-deficient mammalian cells exhibit only a modest delay in disulfide bond formation. To identify *ERO1*-independent pathways to disulfide bond formation, we purified PDI oxidants with a trapping mutant of PDI. PRDX4 stood out in this list, as the related cytosolic peroxiredoxins are known to form disulfides in the presence of hydroperoxides. Mouse embryo fibroblasts lacking *ERO1* were intolerant of PRDX4 knockdown. Introduction of wildtype mammalian PRDX4 into the ER rescued the temperature-sensitive phenotype of an *erol* yeast mutation. In the presence of an H<sub>2</sub>O<sub>2</sub> generating system, purified PRDX4 oxidized PDI and reconstituted oxidative folding of RNase A. These observations implicate ER localized PRDX4 in a previously unanticipated, parallel, *ERO1*-independent pathway that couples hydroperoxide production to oxidative protein folding in mammalian cells.

### Keywords

protein folding; endoplasmic reticulum; hydrogen peroxide; enzyme analysis – in vitro

<sup>7</sup>Corresponding author: David Ron, University of Cambridge, Institute of Metabolic Sciences, level 4, Addenbrookes Hospital, Box 289, Hills Road, Cambridge, CB2 0QQ, United Kingdom, +44-1223-768940 (office), +44-1223-768639 (fax), +44-7825-201560 (mobile), dr360@medschl.cam.ac.uk.

**Publisher's Disclaimer:** This is a PDF file of an unedited manuscript that has been accepted for publication. As a service to our customers we are providing this early version of the manuscript. The manuscript will undergo copyediting, typesetting, and review of the resulting proof before it is published in its final citable form. Please note that during the production process errors may be discovered which could affect the content, and all legal disclaimers that apply to the journal pertain.

## Introduction

Disulfide bond formation in the endoplasmic reticulum involves the transfer of electrons from the reduced cysteines of unfolded proteins to oxidoreductases of the protein disulfide isomerase (PDI) family. This catalytic cycle is completed by the re-oxidation of the reduced PDIs. Genetic studies in yeast and biochemical analysis *in vitro* have implicated the luminal oxidase ERO1 in PDI re-oxidation and disulfide bond formation (reviewed in: Tu and Weissman, 2004; Sevier and Kaiser, 2008).

Yeast lacking ERO1 are nonviable, indicating that ERO1 is required for the essential process of disulfide bond formation (Frand and Kaiser, 1998; Pollard et al., 1998). Mammals have two genes encoding proteins homologous to yeast ERO1, known as ERO1 $\alpha$  (or *ERO1L*) (Cabibbo et al., 2000) and ERO1 $\beta$  (or *ERO1Lb*) (Pagani et al., 2000). Biochemical studies *in vitro*, and ability to complement the yeast mutation *in vivo* prove that the mammalian proteins too function as ER oxidases, accepting electrons from reduced PDI (Cabibbo et al., 2000; Mezghrani et al., 2001; Appenzeller-Herzog et al., 2008; Baker et al., 2008; Blais et al., 2010).

The two isoforms have different tissue distribution: ERO1 $\alpha$  is broadly expressed, whereas ERO1 $\beta$  expression is greatly enriched in the endocrine pancreas and in immunoglobulin secreting cells (Pagani et al., 2000; Dias-Gunasekara et al., 2005; Zito et al., 2010). Compromise of ERO1 $\beta$  expression in mice delays oxidative folding of proinsulin (Zito et al., 2010). Surprisingly, compounding the loss of ERO1 $\beta$  by loss of ERO1 $\alpha$  does not exacerbate the mild diabetic phenotype or the impaired insulin secretion of the single ERO1 $\beta$  mutant (Zito et al., 2010). Given the critical role of disulfide bond formation in insulin biogenesis (Liu et al., 2007), this observation suggests the existence of pathways to mammalian ER oxidation that function in parallel to ERO1.

Fly genetics too provides evidence for the existence of such parallel pathways. Whilst the single ERO1 gene in that species (known as *kiga*) is essential to animal development, clones of homozygous mutant *kiga* cells are presumably capable of oxidative protein folding, as they expand normally in the wing disc and pupal notum (Tien et al., 2008).

Various processes emerge as candidates for ERO1-independent disulfide bond formation. Early studies had emphasized the potential for selective import of disulfide-bonded glutathione into the ER as a driver of protein oxidation (Hwang et al., 1992). More recently Ruddock and colleagues have called attention to the potential role of direct oxidation of cysteine residues by H<sub>2</sub>O<sub>2</sub> or dehydroascorbate as mechanisms for disulfide bond formation (Karala et al., 2009; Saaranen et al., 2010). The secreted enzymes, QSOX1 and QSOX2 can catalyze the oxidation of cysteines on unfolded proteins, and an ER-localized fraction of QSOX could play a role in ER oxidation (Thorpe and Kodali, 2010). Finally, the vitamin K epoxide reductase can utilize oxidized vitamin K to drive PDI oxidation and thereby promote disulfide bond formation (Li et al., 2010).

Here we report on the application of an unbiased method for uncovering candidates in the parallel ERO1-independent pathway to protein oxidation and in the experimental indictment of the ER localized PRDX4 in that pathway.

## Results

### PRDX4 forms stable complexes with an active-site trapping mutant of PDI

The minimal effect of ERO1 loss of function on disulfide bond formation in higher eukaryotes was previously inferred from indirect measurements (Tien et al., 2008; Zito et

al., 2010). To assess this process directly we monitored the disulfide bond-dependent changes in mobility on non-reducing SDS-PAGE as newly-synthesized immunoglobulin-M monomers progress to dimers and decamers in pulse-chase labeled lipopolysacchride-induced blasts cultured from the spleens of wildtype or compound *Ero1L;Ero1Lb* mutant mice (lacking ERO1 $\alpha$  and ERO1 $\beta$  protein). The rate of progression is nearly indistinguishable in the two genotypes (Fig. 1a), confirming the existence of parallel pathways for disulfide bond formation in the ER of ERO1-deficient cells.

ERO1 accepts electrons directly from the reduced C-terminal active site of PDI (Tsai and Rapoport, 2002; Wang et al., 2009). We reasoned that if a parallel pathway were to exploit a similar step in electron transfer, the acceptor protein (the oxidant of PDI) could be trapped in complex with a mutant PDI that is missing the resolving cysteine of its C-terminal active site. To establish this system, wildtype and single (C400S) and double (C56S; C400S) trapping-mutant Flag-M1 epitope-tagged human PDI proteins were expressed by transient transfection of HEK 293T cells. Cell lysates were prepared in the presence of N-ethyl maleimide, to quench free thiols, and protein complexes were immunopurified by the FLAG-M1 tag. Immunoblot of a reducing gel showed that the C-terminal trapping mutant PDI<sup>C400S</sup> associated with more ERO1 $\alpha$  than the wildtype or the double-mutant PDI<sup>C56S,C400S</sup> (Fig. 1b, upper panel). Immunoblot of the non-reducing gel showed that all the detectable ERO1 $\alpha$  that co-purified with PDI<sup>C400S</sup> was associated in a high molecular disulfide bonded complex (Fig. 1b, lower panel). A species of similar mobility was also detected with the anti-FLAG antibody (Fig. 1b, lower panel). These observations confirmed the utility of the trapping mutant PDI<sup>C400S</sup> in stably associating with a known ER oxidase.

To identify other proteins that may associate with the trapping mutant PDI<sup>C400S</sup> in a disulfide-bonded complex, we excised the region of the non-reducing SDS-PAGE containing the trapped complexes. Following in-gel reduction, alkylation and digestion with trypsin, the peptides eluted from the gel slices were analyzed by LC-MS/MS (Fig. 2a). The corresponding human proteins were sorted based on their Exponentially Modified Protein Abundance Index (emPAI) (Fig. 2b).

Among the high emPAI scoring proteins discovered in complex with PDI, PeRoxireDoXin 4 (PRDX4) seemed the most likely to play a role in ER oxidation: Like other members of the family of 2-cysteine peroxiredoxins, PRDX4 has been reported to reduce H<sub>2</sub>O<sub>2</sub> to water by forming an inter-subunit disulfide bond (Hall et al., 2009; Ikeda et al., 2010; Tavender and Bulleid, 2010). Importantly, PRDX4 has been shown to reside in the ER lumen as a soluble protein (Tavender et al., 2008).

Substantial amounts of endogenous PRDX4 immunoreactivity was recovered in complex with the tagged trapping mutant PDI<sup>C400S</sup> in HEK 293T cells (Fig. 2c). On non-reducing gels the complex migrated slowly, consistent with disulfide bonding (Fig. 2d). The FLAG-M1 epitope of the tagged PDI<sup>C400S</sup> is exposed only after cleavage of the protrypsinogen signal sequence by the ER localized leader sequence peptidase (Brizzard et al., 1994), thus the trapping of endogenous PRDX4 likely reflects an interaction that took place in the lumen of the ER. Based on these hints we hypothesized that PRDX4 may utilize luminal H<sub>2</sub>O<sub>2</sub> to form disulfides that it then passes on to PDI to oxidize ER client proteins.

### **PRDX4 buffers the consequences of ERO1 deficiency in mammalian cells**

PRDX4 is not an essential ER enzyme, as mice with a deletion of the first exon, encoding the signal sequence, are viable and fertile (Iuchi et al., 2009). However, we considered that if PRDX4 contributed significantly to disulfide bond formation, its function might become essential in cells lacking ERO1. Therefore, we compared the effect of PRDX4 knockdown

on survival and growth of mouse embryo fibroblasts derived from wildtype and *Ero1L;Ero1Lb* mutant mice.

Lentiviral vectors carrying a dominant selection marker imparting puromycin resistance were used to transduce small hairpin RNAs targeting mouse PRDX4. In both wildtype and double mutant cells transduction led to marked decline in endogenous PRDX4 signal (Fig. 3a). Selection with puromycin resulted in the growth of a thick carpet of transduced ERO1 wildtype PRDX4 knockdown cells, consistent with the mild phenotype of the PRDX4 mutation in mice. However, transduction of the shRNA to PRDX4 elicited growth of fewer puromycin resistant colonies of *Ero1L;Ero1Lb* double mutant MEFs, indicating that cells lacking ERO1 require PRDX4 for normal growth (Fig. 3b & 3c).

Cellular ultra structure was impaired by PRDX4 shRNA. The mild ER dilation noted basally in the *Ero1L;Ero1Lb* double mutant MEFs was conspicuously enhanced by further compromise of PRDX4 expression (Fig. 3d). Together these observations indicate that PRDX4 has an important role in cells lacking ERO1 and suggest that this essential role is involved in ER homeostasis.

To further characterize the impact of PRDX4 loss in MEFs lacking *ERO1*, we examined their sensitivity to exogenously added dithiothreitol (DTT), a disulfide bond reducing agent. Cells were exposed to a brief 30' pulse of 5 mM DTT followed by washout with fresh media. The cell mass quantified 3 hours later was markedly lower in the ERO1 mutant cells compounded by PRDX4 knockdown (Fig 4a).

ERO1 deficient cells had baseline impairment in collagen secretion (another reflection of ERO1's importance to mammalian physiology) that was further (3.8 fold) compromised by PRDX4 shRNA. A less conspicuous (1.8 fold) impairment of collagen secretion was also noted in ERO1 wildtype PRDX4 shRNA cells (Fig. 4b). Both the secretory defect and the hypersensitivity of cells with a combined deficiency of ERO1 and PRDX4 to DTT mirror the phenotype of yeast deficient in ERO1 (Frand and Kaiser, 1998) and suggest a defect in disulfide bond formation.

To directly assess the impact of PRDX4 knockdown on the redox equilibrium in the ER of ERO1 mutant cells, we transduced cells with FLAG\_M1 tagged, ER localized roGFP-iE. This altered version of the fluorescent protein is engineered to contain two exposed cysteines that form a relatively unstable disulfide with a redox potential of  $-235 \pm 7$  mV. roGFP\_iE is thus suited to report on changes in the redox poise of oxidizing environments such as the ER (Lohman and Remington, 2008). The FLAG\_M1-roGFP\_iE immunopurified from the ER of cells with a combined deficiency of ERO1 and PRDX4 was predominantly reduced (89%), whereas that purified from the ER of cells with intact PRDX4 was a mixture of reduced (55%) and oxidized protein (44%) (Fig 4c & 4d). Because the FLAG\_M1 antibody only detects FLAG\_roGFP\_iE after signal peptide cleavage, this assay is not influenced by variation in the efficiency with which the protein translocates into the ER and our observations strongly support an oxidative defect in ERO1 mutant cells lacking PRDX4.

### **ER localized, enzymatically-active PRDX4 rescues a lethal mutation of yeast ERO1**

Yeast lack a known ER localized peroxiredoxin. Therefore we asked if introducing mammalian PRDX4 into the yeast ER could rescue the lethal phenotype of a strong *ERO1* mutation. The FLAG-M1 tagged coding sequence of mature mouse PRDX4 was fused in frame to the cleavable yeast pro-alpha mating factor signal sequence, and the chimeric protein was expressed from the yeast CUP1 promoter as a plasmid episome. Upon transduction of this plasmid, haploid yeast with the highly penetrant temperature-sensitive *ero1-1* mutation (Frand and Kaiser, 1998) acquired the ability to grow at the non-permissive

temperature (Fig. 5a). Expression of PRDX4 had no deleterious effect on growth at the permissive temperature, whereas the growth of the rescued *ero1-1* yeast at the non-permissive temperature approached their growth rate at the permissive temperature (Fig. 5b).

Basal activity of the *CUP1* promoter was sufficient; addition of copper did not enhance the rescue. To confirm that the robust rescue noted above was imparted by persistent expression of the PRDX4 plasmid, we exploited the fact that the *URA3(+)* auxotrophic marker can be used for both positive and negative selection for the presence of the plasmid. *URA3* deficient parental and *ero1-1* yeast that had been transformed by the empty pRS316 or the PRDX4-expressing plasmid were selected for presence of the plasmid in media lacking uracil at the permissive temperature. They were then spotted onto SD plates that either did or did not contain 5' fluoroorotic acid (FOA), which is converted to the toxin 5' fluorouracil by orotidine-5'-phosphate decarboxylase, (encoded by *URA3*). At the permissive temperature both the wildtype and the *ero1-1* mutant yeast rid themselves of the *URA3*<sup>+</sup> PRDX4 expression plasmid and survived the FOA selection. However at the non-permissive temperature only the wildtype yeast grew on FOA (Fig. 5c). These findings indicate that rescue of *ero1-1* is due to persistent expression of the PRDX4 expression plasmid.

In addition to their thiol-mediated peroxidase activity, members of the peroxiredoxin family also have chaperone activity (Hall et al., 2009). To determine if the rescue of the growth defect of *ero1-1* mutant is mediated by the peroxidase activity or the chaperone activity, we mutated the two active site cysteines of PRDX4 in the yeast expression plasmid. To test if localization to the ER is required for rescue, we removed the signal sequence from the protein. All three mutants were well expressed in the *ero1-1* yeast, but only the ER-localized wildtype PRDX4 rescued the temperature sensitive phenotype of the *ero1-1* mutant (Fig. 5d).

We were unable to come to a firm conclusion in regard to the source of H<sub>2</sub>O<sub>2</sub> driving oxidation of PRDX4 in yeast or in mammalian cells. Respiratory deficient *ero1-1* yeast compromised by deletion of *coq3* were nonetheless rescued by PRDX4, indicating that an intact respiratory chain is not a requisite for PRDX4-mediated oxidation in yeast (supplement a to figure 5). Similarly, ERO1 deficient MEFs are not conspicuously hypersensitive to compromise of mitochondrial gene expression by culture in media containing ethidium bromide, nor are they hypersensitive to Diphenylene iodonium (DPI), an inhibitor of NADPH oxidase (data not shown). Finally, this theme of redundancy in H<sub>2</sub>O<sub>2</sub> source(s) is also reflected by the apparent lack of effect of ERO1 genotype on the rate of endogenous PRDX4 re-oxidation following a pulse of DTT (supplement b to figure 5)

### PRDX4 catalyzes H<sub>2</sub>O<sub>2</sub> and PDI-dependent oxidative refolding of RNase A in vitro

Ruddock and colleagues have discovered that H<sub>2</sub>O<sub>2</sub> can directly serve as an electron acceptor in PDI-mediated oxidative refolding of RNase A in vitro (Karala et al., 2009). Ability of PRDX4 to accelerate this thermodynamically-favored process would serve as a strong test of the hypothesis that PRDX4 accelerates disulfide bond formation by converting hydroperoxides to disulfides in the ER lumen.

First we tested PDI's ability to be oxidized by PRDX4, in vitro. Bacterially expressed PDI (150 μM) was reduced by DTT, desalted by gel filtration and reacted with bacterially expressed wildtype PRDX4 (5 μM) or the active site mutants PRDX4<sup>C127S</sup> and PRDX4<sup>C248S</sup> in the absence or presence of an H<sub>2</sub>O<sub>2</sub> generating system consisting of glucose (2.5 mM) and glucose oxidase (10 mu/mL) (Fig. 6a). The time-dependent oxidation of free thiols was assessed by loss of their reactivity with the Ellman reagent (5,5'-dithiobis(2-nitrobenzoate), DTNB). Oxidation was dependent on a source of H<sub>2</sub>O<sub>2</sub> and was accelerated by wildtype PRDX4 but not by the two active-site mutants (Fig. 6b). In the absence of PDI,



PRDX4 was unable to oxidize reduced glutathione, indicating selectivity for the source of electrons in this reaction (Fig 6c)

To determine if the accelerated oxidation of PDI would give rise to accelerated oxidation of reduced and denatured RNase A, we monitored the latter's mobility on non-reduced SDS-PAGE at different time point in an in vitro re-folding reaction. In reactions containing an H<sub>2</sub>O<sub>2</sub> generating system, PRDX4 and PDI, the low mobility, reduced RNase A was rapidly converted to a high mobility form that co-migrated with native RNase A. Omitting any of the three components markedly attenuated this conversion and active site mutants of PRDX4 were ineffective (Fig. 6d). These observations indicate that efficient PRDX4-mediated oxidative folding of RNase A requires active peroxiredoxin, an electron acceptor (H<sub>2</sub>O<sub>2</sub>, in this case) and an oxidoreductase (PDI).

To determine if the refolded RNase A was functional, or whether PRDX4-mediated refolding favored scrambled RNase A, we monitored RNase A enzymatic activity using cyclic cytidine 5'-monophosphate (cCMP) as a substrate (Lyles and Gilbert, 1991). The time-dependent acquisition of RNase A activity correlated well with the rate of refolding on the SDS-PAGE, indicating that the disulfide bonds formed in the presence of PRDX4 and PDI are native (Fig. 6e). Together these observations establish that PRDX4 possesses the enzymatic activity require to substitute for the lack of ERO1.

## Discussion

We have discovered that PRDX4 buffers the growth-inhibitory consequences of ERO1 deficiency in settings ranging from yeast to cultured mouse cells. Such buffering requires expression of PRDX4 in the lumen of the ER and is dependent on the two cysteines of PRDX4 that are involved in its peroxidase activity. In vitro, PRDX4 is able to accelerate the H<sub>2</sub>O<sub>2</sub>-dependent oxidative folding of reduced and denatured RNase A in the presence of PDI. Together, these observations point to an unanticipated role for PRDX4 in converting ER luminal H<sub>2</sub>O<sub>2</sub> to disulfides and in handing these disulfides over to PDI for oxidation of newly synthesized secretory proteins (Fig. 7).

Neither yeasts nor worms, species in which ERO1 is essential (Frand and Kaiser, 1998; Pollard et al., 1998), have genes encoding predicted ER-localized peroxiredoxins. Whereas more complex eukaryotes, such as flies and mice, in which ERO1 is not essential to cell viability, have PRDX4 genes. This correlation, together with the relatively broad expression of PRDX4 in mouse tissues (Iuchi et al., 2009) and the ability of PRDX4 to rescue ERO1 deficiency in the heterologous yeast system, suggests that PRDX4 may be broadly implicated in the observed redundancy of ERO1 in higher eukaryotes.

Peroxiredoxins are pentamers of homodimers. Their catalytic mechanism entails a nucleophilic attack by a peroxidic cysteine (C127, in mouse PRDX4) on a hydroperoxide (likely H<sub>2</sub>O<sub>2</sub>), leading to the formation of a sulfenic acid intermediate that is resolved by a second active site cysteine (C248) from an adjoining protomer. The resulting inter-subunit disulfide is later reduced by a thioredoxin-like protein, completing the catalytic cycle (Hall et al., 2009). Our in vitro studies and the crystal structure of human PRDX4 in the reduced state (PDB:2PN8) are both consistent with this catalytic mechanism and indicate that unlike ERO1, PRDX4 cannot utilize molecular oxygen as the electron acceptor and must instead rely on a source of hydroperoxides.

ERO1 generates one molecule of H<sub>2</sub>O<sub>2</sub> for every disulfide bond formed (Gross et al., 2006). Recent measurements suggest that despite being a non-polar molecule and thus freely diffusible across membranes, H<sub>2</sub>O<sub>2</sub> produced in the ER by ERO1 activity is consumed in that compartment (Enyedi et al., 2010). PRDX4 would be well positioned to use that

peroxide to generate another pair of disulfides, enhancing the efficiency of oxidative protein folding (Fig. 7). Such an arrangement would have the additional benefit of reducing reactive  $H_2O_2$  to water, as suggested by Bulleid and colleagues (Tavender and Bulleid, 2010). In this vein, it is interesting to note that in worms and yeast, which lack a PRDX4-mediated pathway to eliminate ERO1-generated  $H_2O_2$ , attenuation of ERO1 activity provides some protection against the lethality of severe unfolded protein stress in the ER (Haynes et al., 2004; Marciniak et al., 2004). However, no such benefit was observed in the insulin producing  $\beta$ -cells of the mouse pancreas, which have ample PRDX4 (Zito et al., 2010, and unpublished observations). This suggests that the high levels of PRDX4 in the pancreas (Iuchi et al., 2009) and  $\beta$  cells efficiently scavenge and utilize the  $H_2O_2$  produced by ERO1.

Clearly a different source of  $H_2O_2$  is driving PRDX4-dependent disulfide bond formation in cells lacking ERO1. Mitochondria are candidates, and their involvement may explain previous reports of mitochondrial respiration-dependent production of disulfides in mammalian cells (Yang et al., 2007). Junctions known to exist between mitochondria and ER membranes (Kornmann et al., 2009) could serve to channel  $H_2O_2$  into the ER (and away from cytosolic peroxiredoxins) to be used for PRDX4-mediated oxidative protein folding (Fig 7).

In  $\beta$  cells, the tight coupling of mitochondrial respiration to nutrient availability may provide a mechanism for accelerated disulfide bond formation during pro-insulin synthesis, as the latter is translationally activated by nutrients (Itoh and Okamoto, 1980). Such an arrangement may also clarify an interesting peculiarity of  $\beta$  cells in that they contain superoxide dismutases (that convert oxygen radicals to  $H_2O_2$ ) but lack glutathione peroxidase or catalase activity to break down  $H_2O_2$  (Tiedge et al., 1997). This feature may have evolved to enable  $\beta$  cells to efficiently harness  $H_2O_2$  for disulfide bond formation required during pro-insulin folding.

$H_2O_2$  may also be produced by NADPH oxidases. The latter are integral membrane proteins activated post-translationally by a variety of signals, including growth factor receptors (Goldstein et al., 2005). Cytosolic peroxiredoxins channel the  $H_2O_2$  produced by NADPH oxidases to regulate the activity of signaling molecules such as oxidation-sensitive phosphatases (Woo et al., 2010). It is tempting to speculate that a conceptually-similar diffusion of  $H_2O_2$  into the ER from ER localized NADPH oxidases may couple extra-cellular signaling to ER protein oxidation.

Two-cysteine peroxiredoxins are subject to inactivation by formation of a sulfinic acid on the peroxidic cysteine. In the cytosol this reaction is reversed by a sulfiredoxin that reduces the sulfinic acid in an ATP-dependent reaction (Biteau et al., 2003). There are no known sulfiredoxins in the ER, suggesting that inactivation of PRDX4 by formation of a cysteine-sulfinic acid might be irreversible (Tavender and Bulleid, 2010). Such irreversible inactivation of PRDX4 by excess  $H_2O_2$  may account for the seemingly paradoxical induction of unfolded protein stress in the ER under hyperoxidizing conditions and its relief by anti-oxidants (Malhotra et al., 2008). Alternatively, inactivation of PRDX4 by elevated levels of  $H_2O_2$  may regulate the disulfide-based redox poise of the ER, akin to the allosteric inhibition of ERO1 by oxidized PDI (Sevier et al., 2007).

Our discovery of a PRDX4-dependent pathway operating in parallel to ERO1-mediated protein oxidation in the ER does not preclude the existence of other parallel pathways that might be revealed by the phenotype of compound ERO1 and PRDX4 deficiency in other systems. Regardless of whether further redundancy exists, this study points to an unanticipated level of complexity of oxidative protein folding in higher eukaryotes, and suggests a mechanism for regulating this conserved process by the availability of  $H_2O_2$ .

## Materials and methods

### Isolation, culture and metabolic labeling of LPS Blasts

Splenic cells from wildtype and compound homozygous *Ero1a;Ero1b* mutant mice (Zito et al., 2010) were cultured in RPMI-1640 at a density of  $10^6$  cells/ml and exposed to 50  $\mu\text{g/ml}$  Lipopolysaccharide from *E. Coli* (Sigma, L2755) for 2–3 days. Following a 15 min labeling pulse with 60  $\mu\text{Ci/mL}$  of [ $^{35}\text{S}$ ]methionine/cysteine (Perkin Elmer; specific activity,  $>1,000$  Ci/mmol), a cold chase was performed in complete media followed by lysis and immunopurification of the radiolabeled IgM using 5  $\mu\text{L}$  of rabbit anti-mouse IgM (Rockland). Immunoprecipitated proteins were resolved on reducing and non-reducing 10% SDS-PAGE and revealed by autoradiography with a Typhoon Phosphoimager<sup>TM</sup> (GE Healthcare).

### Immunopurification of complexes trapped by FLAG-PDI

Expression plasmids encoding ER localized, N-terminally FLAG-tagged human PDI (PDIA1,18–508) were constructed in the pFLAG-CMV1 vector (Sigma). The C-terminal FLAG-PDI<sup>C400S</sup> and double trapping mutant FLAG-PDI<sup>C56S;C400S</sup>, were made by QuiKChange site direct mutagenesis (Stratagene). Transfected HEK 293T cells from four confluent 100 mm plates, were washed in PBS with 20 mM N-Ethyl Maleimide (NEM), lysed in 0.3% Triton X100, 150mM NaCl, 20 mM Hepes pH 7.4, 10mM CaCl<sub>2</sub>, 20 mM NEM and protease inhibitors). The Flag-tagged proteins were immunopurified with Flag M1 affinity gel (Sigma) in an overnight incubation, eluted in 10 mM EDTA, 20 mM Tris pH 7.5 and 0.002% Tween 20. 10% of the eluted material was immunoblotted with anti Flag M2 (Sigma), rabbit anti ERO1 $\alpha$  antiserum (Zito et al., 2010) or rabbit anti PRDX4 (a gift of Junichi Fujii) (Matsumoto et al., 1999) following reducing and non-reducing SDS-PAGE. The residual 90% was resolved on non-reducing SDS-PAGE stained lightly with Coomassie and the region of the gel containing complexes larger than the FLAG-PDI<sup>C400S</sup> bait, were excised, reduced in 10 mM DTT, alkylated with 20 mM NEM and analyzed by mass spectroscopy.

### Mass spectroscopy

A LTQ-Orbitrap (ThermoFisher, Bremen, Germany) equipped with a nano-ESI source was used for all analyses. Samples were directly infused via a Eksigent 2DLC system (Eksigent Technologies, Dublin, CA) equipped with a 12 cm PicoFrit self-packed column PicoTip emitter (75  $\mu\text{m}$  ID, 10  $\mu\text{m}$  tip diameter from New Objective, Woburn, MA) packed in house with ReproSil-Pur C18-AQ beads (3  $\mu\text{m}$  from Dr. Masch GmbH, Ammerbuch, Germany). Samples were applied with direct loading onto the analytical column (0.8  $\mu\text{L/min}$  for 25 min with mobile phase A; 0.1% formic acid). The flow rate was then changed to 0.3  $\mu\text{L/min}$  and peptides eluted with a gradient of 1–76 % acetonitrile in 0.1 % formic acid over 120 min. Mass spectra were acquired in data dependant mode with one 60 000 resolution MS survey scan in the Orbitrap followed by and up to nine subsequent MS/MS scans in the LTQ from the nine most intense peaks detected in the survey scan. MS survey scans were acquired in profile mode and the MS/MS scans in centroid mode.

Generic MASCOT format files were generated from raw data using DTA SuperCharge (version 2.0a7) and searched using MASCOT software (version 2.3, Matrix Science, London, UK). The human IPI database was searched with peptide mass tolerance 20 ppm and fragment mass tolerance 0.6 Da. Trypsin specificity was set to a maximum of one missed cleavage and N-ethyl maleimide (C), N-ethyl maleimide+water (C) and oxidation (M) were set as variable modifications.



## Lentiviral transduction and analysis of wildtype and *Ero1 $\alpha$* ;*Ero1 $\beta$* mutant MEFs

Wildtype and compound homozygous *Ero1 $\alpha$* ;*Ero1 $\beta$*  mutant mouse embryonic fibroblasts (MEFs), isolated at embryonic day 13.5, were immortalized with SV-40 large T antigen and cultured in DMEM supplemented with 25 mM glucose, 10% FCS and non essential aminoacids. *Prdx4* knockdown was achieved using Mission™ shRNA-encoding lentiviruses directed to mouse *Prdx4* mRNA (Sigma SHCLNG-NM\_016764) following the manufacture's instructions. Knockdown clone KD1 was targeted with shRNA TRCN0000055339, KD2 with TRCN0000055341 and KD3 TRCN0000055339. Following transduction and selection with puromycin at 4  $\mu$ g/ml for two weeks, the cells (in triplicate plates) were fixed, stained with crystal violet and photographed. KD2 had off-pathway toxicity and was not used in the phenotypic analysis. Cell mass was quantified by solubilizing the dye in 0.2% Triton X-100 and measuring the absorbance at 590 nm.

To assess the extent of knockdown achieved  $5 \times 10^6$  cells were transduced, selected for 4 days with puromycin (a period sufficient to kill more than 95% of the non-transduced cells) and the cell lysate was immunoblotted for PRDX4.

Secretion of soluble collagen was measured in the 24 hour conditioned media of MEFs using the Sircol™ colorimetric assay (Biocolor, Ireland) according to the manufacturer's instruction. MEFs were cultured in media with 10% FCS for 48h before the assay and switched to media with 0.5% FCS to collect the conditioned media. The sensitivity of cells to reductive stress was measured by crystal violet staining of the cell mass that remained on the plate 3 hours after a 30 minutes challenge with 5 mM DTT.

The roGFP\_iE cDNA (Lohman and Remington, 2008) was ligated in frame with the FLAG\_M1 tag in a lentiviral vector to transduce cells of the indicated genotype. Cells were lysed in the presence of 20 mM N-ethyl maleimide and the FLAG\_M1-roGFP\_iE was immunoprecipitated with the FLAG-M1 monoclonal antibody, resolved on 15% SDS-PAGE in the absence or presence of DTT and blotted with FLAG M2

Cell pellets were fixed by immersion in 2% glutaraldehyde and 2.0% paraformaldehyde in 0.1M sodium cacodylate buffer (pH 7.2), postfixed in 1% osmium tetroxide, and en bloc stained with 1% uranyl acetate. The sample was dehydrated in ethanol embedded in Epon (Electron Microscopy Sciences, Hatfield, PA). Ultrathin sections were poststained with uranyl acetate and lead citrate and examined using an electron microscope (CM12, FEI, Eindhoven, The Netherlands) at 120 kV. Images were recorded digitally using a camera system (Gatan 4k  $\times$  2.7K) with software Gatan DigitalMicrograph (Gatan Inc., Pleasanton, CA).

## Yeast strains and plasmids

The temperature sensitive yeast strain CKY598 bearing the *ero1-1* mutation (C. Kaiser lab at MIT) and the wild type strain were transformed with PRDX4-pRS316, in which the cleavable yeast  $\alpha$  mating factor signal sequence is fused in frame with FLAGM1-tagged mature wildtype or active site mutant mouse PRDX4(37–274) and expression driven by the yeast *CUP1* promoter and termination sequences from the *CPY1* gene. A cytosolic version was made by replacing the yeast  $\alpha$  mating factor signal sequence with an initiator methionine (yielding a protein nearly identical in size to mature ER version). Transformed yeast were selected on minimal media lacking uracil or SD media with and without 0.1% 5' fluoroorotic acid (FOA) (Sigma) and incubated at the permissive (24 °C) or non-permissive temperature (37 °C).

## Protein oxidation in vitro

Mouse PRDX4<sup>WT</sup> and the mutants PRDX4<sup>C127S</sup> and PRDX4<sup>C248S</sup> were expressed as a GST fusion proteins in *E. coli* Rosetta (D3) strain followed by glutathione affinity chromatography and gel filtration on Superdex 200. Human PDI (PDIA1 18–508, a gift of C. Thorpe, University of Delaware), was expressed in *E. coli* BL21 (D3) strain, purified with Ni-NTA affinity chromatography and dialyzed into the reaction buffer.

PDI was reduced by incubation with 50mM of DTT, 1h at room temperature, and then desalted on PD-10 gel filtration column (GE Healthcare). Oxidation in vitro was performed in the presence of glucose (2.5 mM) and glucose oxidase (10 mu/mL) type II from *Aspergillus niger* (Sigma) in 80 mM sodium phosphate, pH=7.0. Where indicated reduced glutathione was added to the reaction. Free thiols were quantified at different time points by combining 100  $\mu$ L of 0.5 mM Ellman's reagent (5,5'-dithiobis-(2-nitrobenzoic acid) with 30  $\mu$ L of sample and absorbance at 405 nm measured in a Tecan Infinite 500 plate reader. In some assays reduced glutathione was added as an upstream electron acceptor.

RNase A (from bovine pancreas, Roche) was reduced and denaturated overnight in the presence of 6 M guanidinium hydrochloride and 140 mM DTT in 50 mM phosphate buffer, pH 7 and desalted into the assay buffer on PD-10 column before run the refolding assays. Reduced RNase A (25  $\mu$ M) was then incubated with PDI (7  $\mu$ M) and PRDX4 (5 $\mu$ M) in the presence of glucose (2.5 mM) and glucose oxidase (10 mu/mL) in 80 mM phosphate buffer, pH 7. Aliquots of 20  $\mu$ L were withdrawn at different time points reacted with 2  $\mu$ L of 0.5 M N-ethyl maleimide (NEM) for 15' on ice. Refolding of RNaseA was then analyzed on an 18% Tris-tricine gels under non-reducing conditions.

The functional state of RNase A was measured by adding cytidine 2',3' cyclic monophosphate monosodium salt (cCMP from Sigma) and reading the development of absorbance from its hydrolytic product at 296 nm, in a temperature controlled Agilent diode array spectrophotometer at 25°C, as described (Lyles and Gilbert, 1991)

## Statistical Analysis

All results are expressed as means  $\pm$  SEM. Two-tailed Student's T tests were performed to determine p values for paired samples, and two-way ANOVA for the experiments that employ more than one independent variable.

## Supplementary Material

Refer to Web version on PubMed Central for supplementary material.

## Acknowledgments

We thank C. Sevier and C. Kaiser (Massachusetts Institute of Technology) for the CKY598 *ero1-1* mutant yeast and advice on its use. A. Liang and E. Roth from the imaging core facility of NYU School of Medicine for processing and acquiring the EM images. J. Fujii (Yamagata University) for the antiserum to PRDX4, C. Thorpe (University of Delaware) for the gift of the PDI expression plasmid, J. Remington (University of Oregon) for the roGFP\_iE and A. Tzagaloff (Columbia University) for the *coq3* deleted yeast and advice on its use, M. (University of Toronto) for the *sec72 $\Delta$ ;ero1-1* compound haploid and H. Klein and A. Epshtein (NYU) for advice and help with yeast genetics.

Supported by an EMBO long-term fellowship ALTF649-2008 to EZ, Fundação para a Ciência e Tecnologia, Portugal (SFRH/BSAB/922/2009, PTDC/QUI/73027/2006 and IBB/CBME LA) to EPM and by NIH grants DK47119, DK075311 and ES08681 to DR and NS050276, CA016087 & a grant from the 100 Women In Hedge Funds Foundation to TAN. DR is a Wellcome Trust Principal Research Fellow.

## References

- Appenzeller-Herzog C, Riemer J, Christensen B, Sorensen ES, Ellgaard L. A novel disulphide switch mechanism in Ero1alpha balances ER oxidation in human cells. *EMBO J.* 2008; 27:2977–2987. [PubMed: 18833192]
- Baker KM, Chakravarthi S, Langton KP, Sheppard AM, Lu H, Bulleid NJ. Low reduction potential of Ero1alpha regulatory disulphides ensures tight control of substrate oxidation. *EMBO J.* 2008; 27:2988–2997. [PubMed: 18971943]
- Biteau B, Labarre J, Toledano MB. ATP-dependent reduction of cysteine-sulphinic acid by *S. cerevisiae* sulphiredoxin. *Nature.* 2003; 425:980–984. [PubMed: 14586471]
- Blais JD, Chin KT, Zito E, Zhang Y, Heldman N, Harding HP, Fass D, Thorpe C, Ron D. A small molecule inhibitor of endoplasmic reticulum oxidation 1 (ERO1) with selectively reversible thiol reactivity. *J Biol Chem.* 2010 E-published 100506.
- Brizzard BL, Chubet RG, Vizard DL. Immunoaffinity purification of FLAG epitope-tagged bacterial alkaline phosphatase using a novel monoclonal antibody and peptide elution. *Biotechniques.* 1994; 16:730–735. [PubMed: 8024796]
- Cabibbo A, Pagani M, Fabbri M, Rocchi M, Farmery MR, Bulleid NJ, Sitia R. ERO1-L, a human protein that favors disulfide bond formation in the endoplasmic reticulum. *J Biol Chem.* 2000; 275:4827–4833. [PubMed: 10671517]
- Dias-Gunasekara S, Gubbens J, van Lith M, Dunne C, Williams JA, Katakly R, Scoones D, Laphorn A, Bulleid NJ, Benham AM. Tissue-specific expression and dimerization of the endoplasmic reticulum oxidoreductase Ero1beta. *J Biol Chem.* 2005; 280:33066–33075. [PubMed: 16012172]
- Enyedi B, Varnai P, Geiszt M. Redox State of the Endoplasmic Reticulum Is Controlled by Ero1L-alpha and Intraluminal Calcium. *Antioxid Redox Signal.* 2010; 13:721–729. [PubMed: 20095866]
- Frاند AR, Kaiser CA. The ERO1 gene of yeast is required for oxidation of protein dithiols in the endoplasmic reticulum. *Mol Cell.* 1998; 1:161–170. [PubMed: 9659913]
- Goldstein BJ, Mahadev K, Wu X, Zhu L, Motoshima H. Role of insulin-induced reactive oxygen species in the insulin signaling pathway. *Antioxid Redox Signal.* 2005; 7:1021–1031. [PubMed: 15998257]
- Gross E, Sevier CS, Heldman N, Vitu E, Bentzur M, Kaiser CA, Thorpe C, Fass D. Generating disulfides enzymatically: reaction products and electron acceptors of the endoplasmic reticulum thiol oxidase Ero1p. *Proc Natl Acad Sci U S A.* 2006; 103:299–304. [PubMed: 16407158]
- Hall A, Karplus PA, Poole LB. Typical 2-Cys peroxiredoxins--structures, mechanisms and functions. *FEBS J.* 2009; 276:2469–2477. [PubMed: 19476488]
- Haynes CM, Titus EA, Cooper AA. Degradation of misfolded proteins prevents ER-derived oxidative stress and cell death. *Mol Cell.* 2004; 15:767–776. [PubMed: 15350220]
- Hwang C, Sinskey AJ, Lodish HF. Oxidized redox state of glutathione in the endoplasmic reticulum. *Science.* 1992; 257:1496–1502. [PubMed: 1523409]
- Ikeda Y, Ito R, Ihara H, Okada T, Fujii J. Expression of N-terminally truncated forms of rat peroxiredoxin-4 in insect cells. *Protein Expr Purif.* 2010; 72:1–7. [PubMed: 20144717]
- Ishihama Y, Oda Y, Tabata T, Sato T, Nagasu T, Rappsilber J, Mann M. Exponentially modified protein abundance index (emPAI) for estimation of absolute protein amount in proteomics by the number of sequenced peptides per protein. *Mol Cell Proteomics.* 2005; 4:1265–1272. [PubMed: 15958392]
- Itoh N, Okamoto H. Translational control of proinsulin synthesis by glucose. *Nature.* 1980; 283:100–102. [PubMed: 6985712]
- Iuchi Y, Okada F, Tsunoda S, Kibe N, Shirasawa N, Ikawa M, Okabe M, Ikeda Y, Fujii J. Peroxiredoxin 4 knockout results in elevated spermatogenic cell death via oxidative stress. *Biochem J.* 2009; 419:149–158. [PubMed: 19105792]
- Karala AR, Lappi AK, Saaranen MJ, Ruddock LW. Efficient peroxide-mediated oxidative refolding of a protein at physiological pH and implications for oxidative folding in the endoplasmic reticulum. *Antioxid Redox Signal.* 2009; 11:963–970. [PubMed: 19117384]

- Kornmann B, Currie E, Collins SR, Schuldiner M, Nunnari J, Weissman JS, Walter P. An ER-mitochondria tethering complex revealed by a synthetic biology screen. *Science*. 2009; 325:477–481. [PubMed: 19556461]
- Li W, Schulman S, Dutton RJ, Boyd D, Beckwith J, Rapoport TA. Structure of a bacterial homologue of vitamin K epoxide reductase. *Nature*. 2010; 463:507–512. [PubMed: 20110994]
- Liu M, Hodish I, Rhodes CJ, Arvan P. Proinsulin maturation, misfolding, and proteotoxicity. *Proc Natl Acad Sci U S A*. 2007; 104:15841–15846. [PubMed: 17898179]
- Lohman JR, Remington SJ. Development of a family of redox-sensitive green fluorescent protein indicators for use in relatively oxidizing subcellular environments. *Biochemistry (Mosc)*. 2008; 47:8678–8688.
- Lyles MM, Gilbert HF. Catalysis of the oxidative folding of ribonuclease A by protein disulfide isomerase: pre-steady-state kinetics and the utilization of the oxidizing equivalents of the isomerase. *Biochemistry (Mosc)*. 1991; 30:619–625.
- Malhotra JD, Miao H, Zhang K, Wolfson A, Pennathur S, Pipe SW, Kaufman RJ. Antioxidants reduce endoplasmic reticulum stress and improve protein secretion. *Proc Natl Acad Sci U S A*. 2008; 105:18525–18530. [PubMed: 19011102]
- Marciniak SJ, Yun CY, Oyadomari S, Novoa I, Zhang Y, Jungreis R, Nagata K, Harding HP, Ron D. CHOP induces death by promoting protein synthesis and oxidation in the stressed endoplasmic reticulum. *Genes Dev*. 2004; 18:3066–3077. [PubMed: 15601821]
- Matsumoto A, Okado A, Fujii T, Fujii J, Egashira M, Niikawa N, Taniguchi N. Cloning of the peroxiredoxin gene family in rats and characterization of the fourth member. *FEBS Lett*. 1999; 443:246–250. [PubMed: 10025941]
- Mezghrani A, Fassio A, Benham A, Simmen T, Braakman I, Sitia R. Manipulation of oxidative protein folding and PDI redox state in mammalian cells. *EMBO J*. 2001; 20:6288–6296. [PubMed: 11707400]
- Pagani M, Fabbri M, Benedetti C, Fassio A, Pilati S, Bulleid NJ, Cabibbo A, Sitia R. Endoplasmic reticulum oxidoreductin 1-beta (ERO1-Lbeta), a human gene induced in the course of the unfolded protein response. *J Biol Chem*. 2000; 275:23685–23692. [PubMed: 10818100]
- Pollard MG, Travers KJ, Weissman JS. Ero1p: a novel and ubiquitous protein with an essential role in oxidative protein folding in the endoplasmic reticulum. *Mol Cell*. 1998; 1:171–182. [PubMed: 9659914]
- Saaranen MJ, Karala AR, Lappi AK, Ruddock LW. The role of dehydroascorbate in disulfide bond formation. *Antioxid Redox Signal*. 2010; 12:15–25. [PubMed: 19686035]
- Sevier CS, Kaiser CA. Ero1 and redox homeostasis in the endoplasmic reticulum. *Biochim Biophys Acta*. 2008; 1783:549–556. [PubMed: 18191641]
- Sevier CS, Qu H, Heldman N, Gross E, Fass D, Kaiser CA. Modulation of cellular disulfide-bond formation and the ER redox environment by feedback regulation of Ero1. *Cell*. 2007; 129:333–344. [PubMed: 17448992]
- Tavender TJ, Bulleid NJ. Peroxiredoxin IV protects cells from oxidative stress by removing H<sub>2</sub>O<sub>2</sub> produced during disulphide formation. *J Cell Sci*. 2010
- Tavender TJ, Sheppard AM, Bulleid NJ. Peroxiredoxin IV is an endoplasmic reticulum-localized enzyme forming oligomeric complexes in human cells. *Biochem J*. 2008; 411:191–199. [PubMed: 18052930]
- Thorpe C, Kodali VK. Oxidative Protein Folding and the Quiescin-sulfhydryl Oxidase Family of Flavoproteins. *Antioxid Redox Signal*. 2010
- Tiedge M, Lortz S, Drinkgern J, Lenzen S. Relation between antioxidant enzyme gene expression and antioxidative defense status of insulin-producing cells. *Diabetes*. 1997; 46:1733–1742. [PubMed: 9356019]
- Tien AC, Rajan A, Schulze KL, Ryoo HD, Acar M, Steller H, Bellen HJ. Ero1L, a thiol oxidase, is required for Notch signaling through cysteine bridge formation of the Lin12-Notch repeats in *Drosophila melanogaster*. *J Cell Biol*. 2008; 182:1113–1125. [PubMed: 18809725]
- Tsai B, Rapoport TA. Unfolded cholera toxin is transferred to the ER membrane and released from protein disulfide isomerase upon oxidation by Ero1. *J Cell Biol*. 2002; 159:207–216. [PubMed: 12403808]

- Tu BP, Weissman JS. Oxidative protein folding in eukaryotes: mechanisms and consequences. *J Cell Biol.* 2004; 164:341–346. [PubMed: 14757749]
- Wang L, Li SJ, Sidhu A, Zhu L, Liang Y, Freedman RB, Wang CC. Reconstitution of human Ero1- $\alpha$ /protein-disulfide isomerase oxidative folding pathway in vitro. Position-dependent differences in role between the a and a' domains of protein-disulfide isomerase. *J Biol Chem.* 2009; 284:199–206. [PubMed: 19001419]
- Woo HA, Yim SH, Shin DH, Kang D, Yu DY, Rhee SG. Inactivation of peroxiredoxin I by phosphorylation allows localized H<sub>2</sub>O<sub>2</sub> accumulation for cell signaling. *Cell.* 2010; 140:517–528. [PubMed: 20178744]
- Yang Y, Song Y, Loscalzo J. Regulation of the protein disulfide proteome by mitochondria in mammalian cells. *Proc Natl Acad Sci U S A.* 2007; 104:10813–10817. [PubMed: 17581874]
- Zito E, Chin KT, Blais J, Harding HP, Ron D. ERO1 $\beta$ , a pancreas-specific disulfide oxidase promotes insulin biogenesis and glucose homeostasis. *J Cell Biol.* 2010; 188:821–832. [PubMed: 20308425]



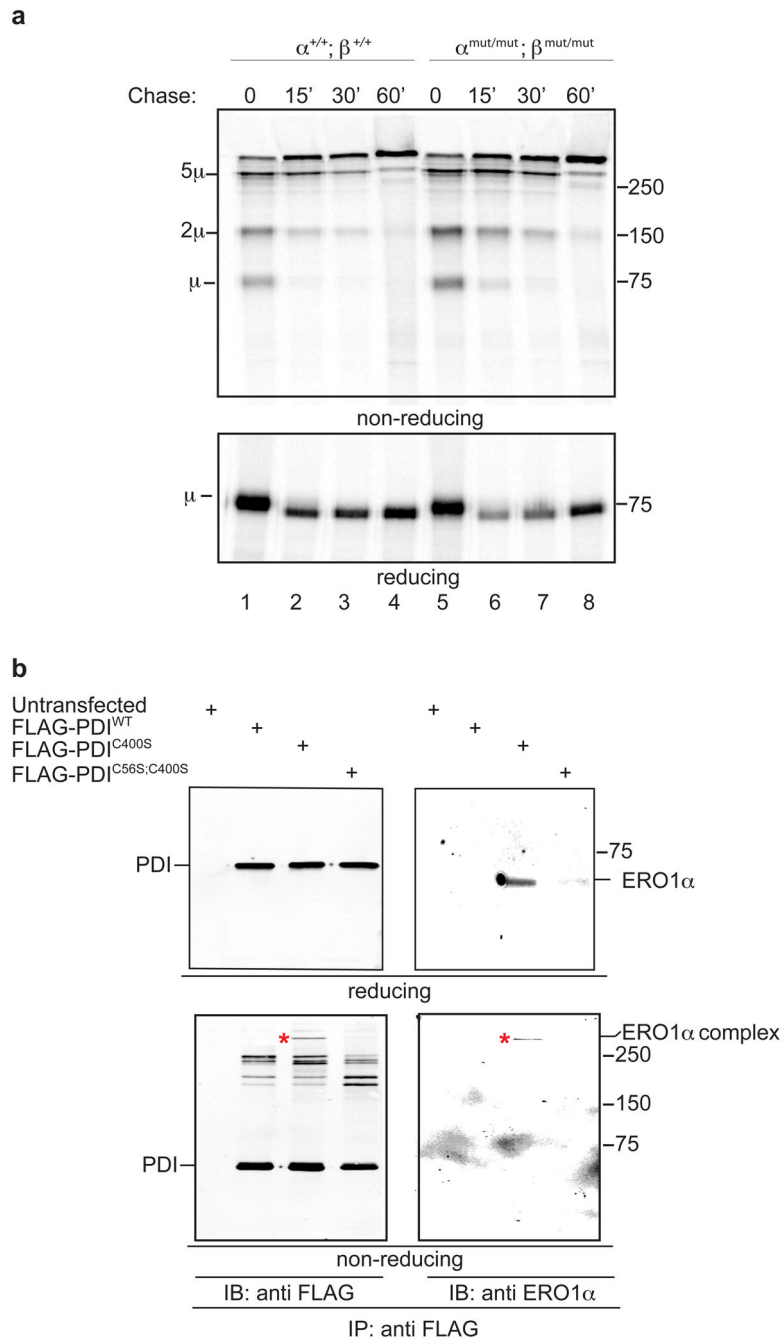


**Figure 1. A trapping mutant of PDI engages the known downstream electron acceptor, ERO1 $\alpha$ , in mammalian cells**

**(a)** Autoradiograph of immunoglobulin-M from metabolically-labeled wildtype ( $\alpha^{+/+}; \beta^{+/+}$ ) and ERO1 mutant ( $\alpha^{\text{mut/mut}}; \beta^{\text{mut/mut}}$ ) lipopolysaccharide blasts. Cells were labeled with  $^{35}\text{S}$  methionine-cysteine for 15 minutes and chased for the indicated time with unlabeled media before lysis and immunoprecipitation. The upper panel is a radiograph of a non-reducing gel and the lower panel is a reducing gel. The migration of IgM monomers ( $\mu$ ) dimers ( $2\mu$ ) and pentamers of dimers ( $5\mu$ ) is indicated.

**(b)** Immunoblots of FLAG-tagged proteins (left) or endogenous ERO1 $\alpha$  (right) immunopurified with the FLAG-M1 antibody from lysates of HEK 293T cells that were

untransfected or transfected with expression plasmids of the indicated proteins. The upper panels are of reducing and the lower panels non-reducing gels. The low mobility complex containing ERO1 $\alpha$  immunoreactive material in complex with the FLAG-tagged PDI C-terminal active site trapping mutant (FLAG-PDI<sup>C400S</sup>) is noted by an asterisks on both non-reducing gels.

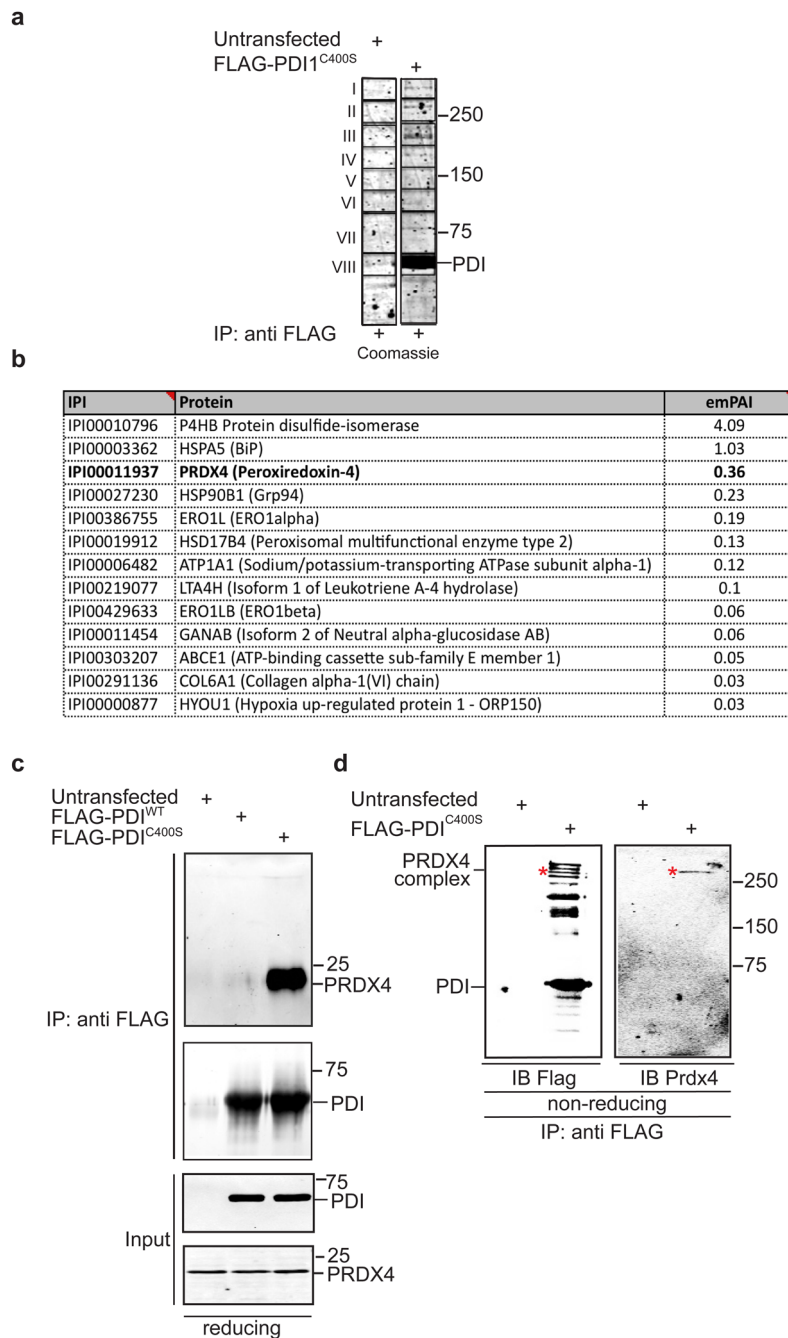


**Figure 2. A PDI active-site trapping mutant engages PRDX4 in mammalian cells**

**(a)** Coomassie stained non-reducing SDS-PAGE of proteins immunopurified in complex with FLAG-tagged PDI trapping mutant from untransfected and transfected cells. The boxes demarcate the binning for the mass spectrometric protein analysis.

**(b)** List of proteins identified by LC MS/MS sequencing of tryptic peptide of endogenous proteins captured in a disulfide linked complex by a FLAG M2-tagged trapping mutant PDI<sup>C400S</sup> expressed in HEK 293T cells (shown in Fig. 2a). Known cytosolic, nuclear and mitochondrial proteins were removed from the list and the remaining proteins were sorted by descending exponentially modified protein abundance index (emPAI) (Ishihama et al.,

2005). The proteins are identified by their International Protein Index accession number (IPI) and their common name.

**(c)** Immunoblot of endogenous PRDX4 and FLAG-tagged wildtype PDI and trapping mutant PDI<sup>C400S</sup> immunopurified with the FLAG-M1 antibody from lysates of HEK 293T cells that were untransfected or transfected with expression plasmids for the indicated proteins. The lower two panels are of the same proteins in the lysates before the IP (“Input”). The proteins shown were resolved on reducing SDS-PAGE

**(d)** FLAG and endogenous PRDX4 immunoblot of a non-reducing gel with samples as in panel “b”. The low mobility complex containing PRDX4 immunoreactive material in complex with FLAG-PDI<sup>C400S</sup> is noted by an asterisks on both non reducing gels.

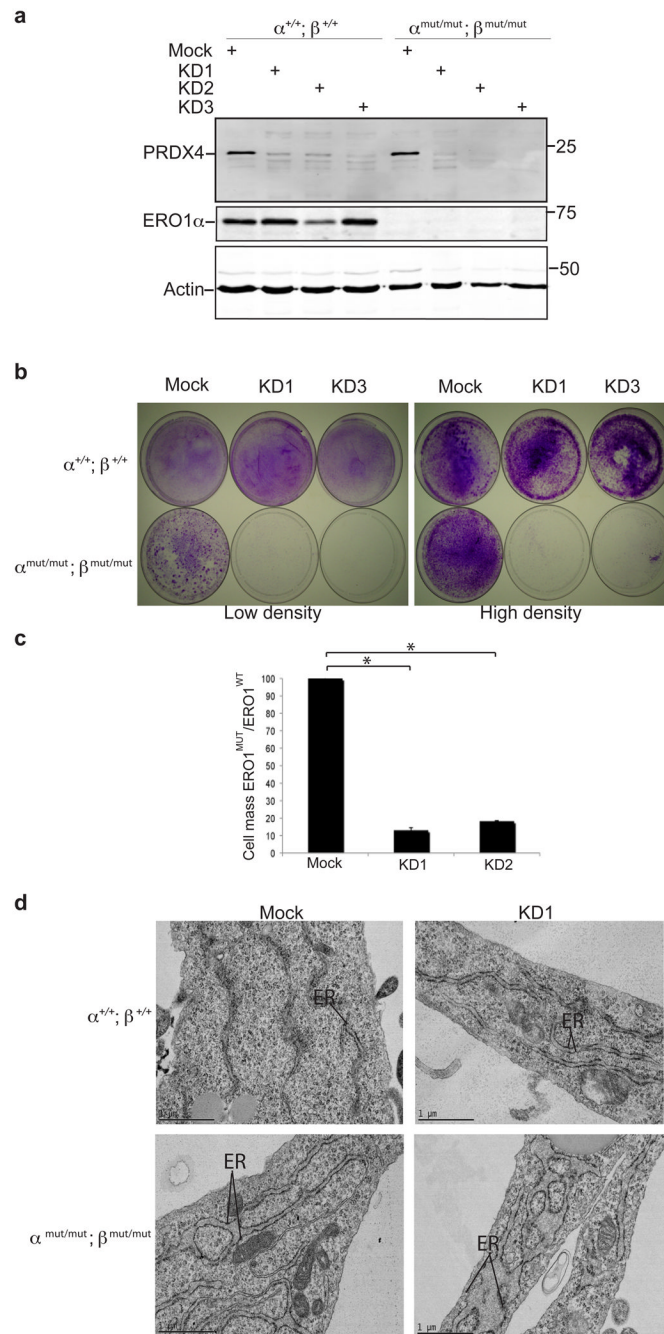


**Figure 3. PRDX4 buffers the consequences of ERO1 deficiency in MEFs**

**(a)** Immunoblot of endogenous PRDX4, ERO1α and Actin in wildtype ( $\alpha^{+/+}; \beta^{+/+}$ ) and ERO1 mutant ( $\alpha^{\text{mut/mut}}; \beta^{\text{mut/mut}}$ ) MEFs 4 days after transduction with a *puro<sup>r</sup>*-marked lentivirus carrying a irrelevant insert (mock) or three different short hairpin RNAs directed to mouse PRDX4.

**(b)** Crystal violet stained plates following two weeks puromycin selection after seeding with  $8 \times 10^3$  (Low density) or  $4 \times 10^4$  (High density) MEFs of the indicated genotype and transduced with *puro<sup>r</sup>*-tagged lentivirus carrying the indicated shRNA.

**(c)** Bar diagram of the ratio of cell mass accrued in the ERO1 double mutant versus wildtype MEFs from the experiment shown in “b”. The ratio was normalized to 1 in the cells



transduced with the irrelevant shRNA. Shown are means  $\pm$  SEM of a typical experiment reproduced three times (n=3, p<0.05)

**(d)** Transmission electron micrographs of MEFs of the indicated genotype following transduction with a lentivirus containing an irrelevant shRNA or an shRNA directed to PRDX4. Note the dilation of the ER in the mutant cells transduced with the shRNA to PRDX4.

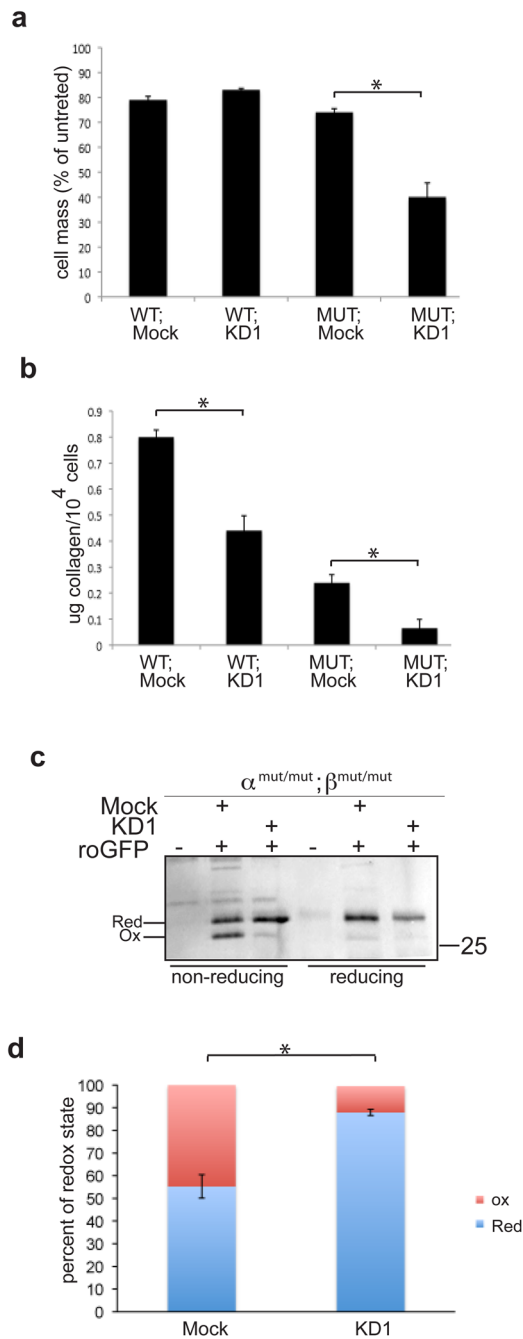


**Figure 4. Hypersensitivity to reducing agents, defective collagen secretion and a more reducing ER redox poise in ERO1-deficient cells lacking PRDX4**

(a) Bar diagram of cell mass of wildtype (WT) or *Ero1 $\alpha^{mut/mut};Ero1\beta^{mut/mut}$*  compound mutant cells (MUT) transduced with mock or PRDX4 RNAi lentivirus (KD1) remaining 3 hours after a 30 minute pulse with DTT (5 mM) followed by recovery in normal media, normalized to the cell mass of a parallel culture of the same cells that had not been exposed to DTT. Shown are aggregate means  $\pm$  SEM from a typical experiment conducted in triplicate (n=3; \*p<0.05) and reproduced three times.

(b) Bar diagram of soluble collagen secreted into the conditioned media from the cells described in panel “a”, normalized to the number of live cells in the culture. Shown are

means  $\pm$  SEM from three experiments conducted on different occasions in triplicate (n=9; \* p<0.01).

**(c)** Immunoblot of FLAG\_M1\_roGFP\_iE immunopurified from the ER of ERO1 deficient MEFs with normal levels of PRDX4 or PRDX4 knockdown. The purified proteins were resolved by SDS-PAGE under non-reducing or reducing conditions. The position of the reduced and oxidized FLAG\_M1\_roGFP\_iE in a typical experiment reproduced three times is shown.

**(d)** Quantitative representation of the data from the experiment represented in panel C. Bar diagram of the ratio of reduced and oxidized roGFP in the *Ero1 $\alpha^{mut/mut}$* ; *Ero1 $\beta^{mut/mut}$*  compound mutant cells transduced with mock or PRDX4 RNAi lentivirus (KD1) (n=3 \*p<0.05, comparing oxidized fraction in the two genotypes)

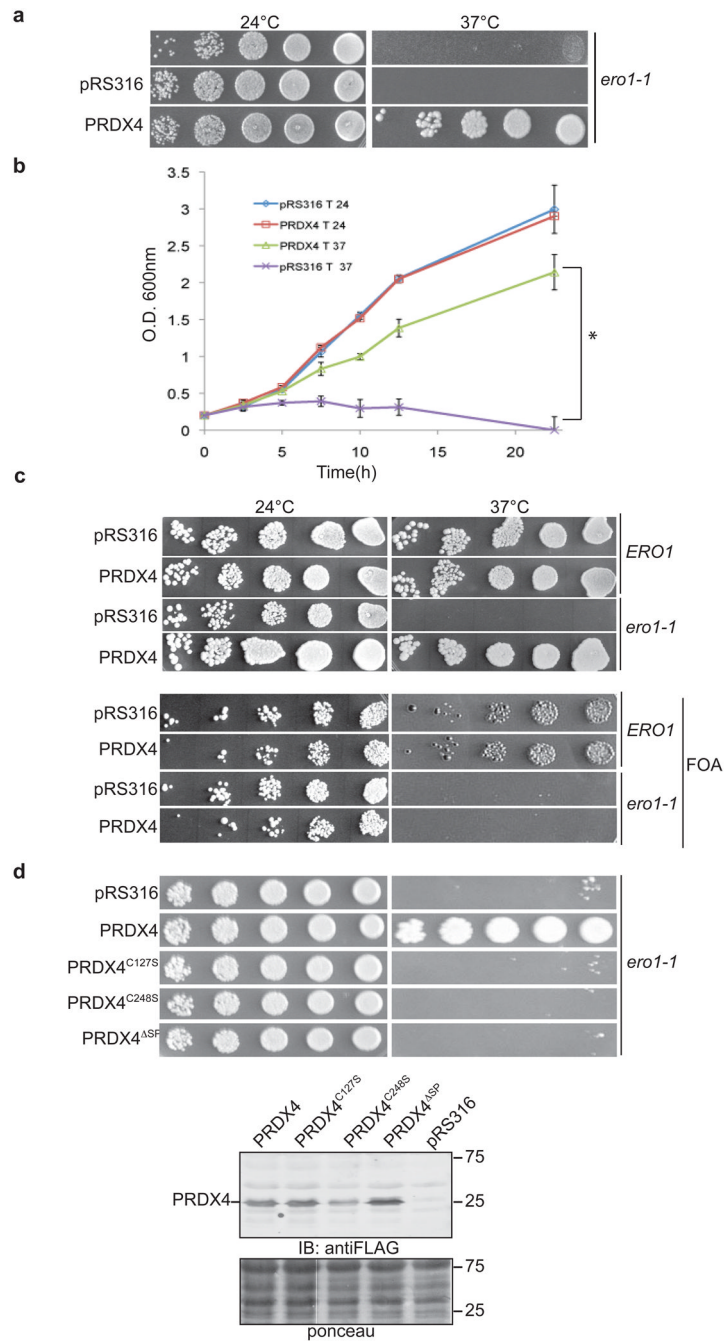


**Figure 5. ER localized, enzymatically-active PRDX4 rescues a lethal mutation of yeast ERO1**

**(a)** Photomicrographs of serial dilutions of untransformed *ero1-1* mutant yeast or transformed with yeast expression plasmids lacking (pRS316) or containing the PRDX4 coding sequence cultured at the permissive temperature of 24°C or the non-permissive temperature of 37°C.

**(b)** Plot of absorbance at 600 nm of cultures inoculated with *ero1-1* yeast transformed with the expression plasmid lacking (pRS316) or containing the PRDX4 coding sequence and cultured at the permissive temperature of 24°C or the non-permissive temperature of 37°C. Shown are mean  $\pm$  SEM of a typical experiment conducted in triplicate (n=3; \* the last four time points  $p < 0.001$  by two-way ANOVA).

**(c)** Photomicrographs of serial dilutions of *ero1-1* yeast transformed with pRS316 or the PRDX4 expressing plasmids and plated in the absence or presence of the toxin FOA at 24°C or 37°C. Note the inability of the *ero1-1* yeast transformed with the PRDX4 expression plasmid to survive on FOA at the non-permissive temperature.

**(d)** Photomicrographs of serial dilutions of *ero1-1* yeast transformed with pRS316 or plasmids expressing wildtype or the indicated mutations in PRDX4 ( $\Delta$ SP: lacks the signal peptide required for ER import of PRDX4). The lower panel is an immunoblot of FLAG-tagged PRDX4 from the four transformed strains and the parental *ero1-1* yeast.





**(c)** Time dependent change in absorbance of Ellman's reagent in reaction mixes containing 150  $\mu\text{M}$  reduced glutathione in the presence of PDI (10  $\mu\text{M}$ ), PRDX4 (5  $\mu\text{M}$ ) or both enzymes. Glucose (2.5 mM) and glucose oxidase (GO, 10 mU/mL) were included as a source of  $\text{H}_2\text{O}_2$  in all reactions. The absorbance of each reaction mixture at  $t=0$  is set at 100%. Shown are means  $\pm$  SEM of a typical assay conducted in triplicate and reproduced 3 times ( $n=3$ ,  $**P<0.001$ ).

**(d)** Coomassie-stained SDS-PAGE of reduced and denatured RNase A (25 $\mu\text{M}$ ) after reacting for the indicated time with reduced PDI (7  $\mu\text{M}$ ) and PRDX4 (5  $\mu\text{M}$ ) in the presence of glucose (2.5 mM) and glucose oxidase (10 mU/mL) as a source of  $\text{H}_2\text{O}_2$ . Lane 13 in the top-most panel or lane 9 in the two lower panels contains a sample of native oxidized RNase A to serve as a reference.

**(e)** Time-dependent change in RNase activity measured spectrophotometrically by absorbance at 296 nm using cCMP (4.5 mM) as substrate. The re-folding of RNase A was initiated at  $t=0$  in reactions as in panel "C". Enzymatic activity of an equal amount of native RNase A is set as 100%. Shown are means  $\pm$  SEM of a typical experiment reproduced 4 times ( $n=3$ , \*  $p<0.05$ , \*\*  $p<0.001$  by two-way ANOVA).

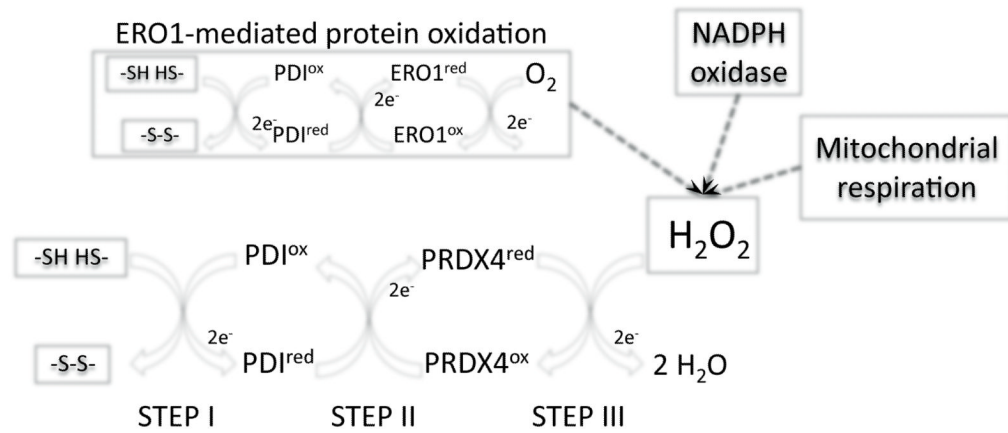


**Figure 7. Model for PRDX4-mediated oxidative protein folding in the ER**

Disulfide bond formation (step I) leaves PDI in a reduced state. PDI is re-oxidized by reducing the active site disulfide (formed between two PRDX4 protomers) in step II. PRDX4 is re-oxidized by interaction of its peroxidic cysteine (C127) with H<sub>2</sub>O<sub>2</sub>, releasing one molecule of water. The sulfenic acid is resolved by C287, regenerating the disulfide and releasing the second molecule of water (step III). PRDX4 may utilize H<sub>2</sub>O<sub>2</sub> produced by ERO1 as well as H<sub>2</sub>O<sub>2</sub> produced by mitochondrial respiration or NADPH oxidases that may diffuse into the ER.